Carbohydrate Polymers 88 (2012) 139–145

Contents lists available at SciVerse ScienceDirect

Carbohydrate Polymers

journal homepage: www.elsevier.com/locate/carbpol

Solution properties and microstructure of cationic cellulose/sodium dodecyl benzene sulfonate complex system

Jing Han, Fa Cheng, Xiangguo Wang, Yuping Wei*

Department of Chemistry, Tianjin University, Tianjin 300072, PR China

ARTICLE INFO

Article history:
Received 17 October 2011
Received in revised form
16 November 2011
Accepted 23 November 2011
Available online 6 December 2011

Keywords:
Cationic cellulose
Micropolarity
Aggregation number
Microstructure

ABSTRACT

In this work, the interactions between cationic cellulose (PQ-10) and anionic surfactant (SDBS) in aqueous media were investigated by turbidity, electric conductivity, steady-state fluorescence, shear rheology and transmission electron microscopy (TEM) analyses. Results indicated that precipitation appeared near the charge neutrality point, and the size of precipitation region widened with increasing PQ-10 concentration (0.57–1.72 mM for 0.05% PQ-10, and 2.30–17.22 mM for 0.5% PQ-10). The specific conductivity values of SDBS in the presence of PQ-10 were higher than that of pure SDBS over the whole concentration range under current experimental conditions. The aggregation number of SDBS kept constant in the flat region of the micropolarity curve (0.86 mM–1.43 mM). The structural transformation of the mixtures was monitored visually by TEM. As SDBS concentration increased, the morphologies of the mixtures changed gradually from branched wormlike aggregates to interconnected networks, finally the networks collapsed.

1. Introduction

Mixing of polymer with surfactant always generates many improved properties or new applications, such as improving oil recovery, loading and releasing drug (Chavanpatil et al., 2007; Scherlund, Brodin, & Malmsten, 2000), isolating and purifying DNA (Mel'nikov, Sergeyev, & Yoshikawa, 1995), acting as simplified model of bio-process (Nilsson, Goldraich, Lindman, & Talmon, 2000), maintaining stability and regulating rheology of cosmetics. Owing to these widespread technical applications especially some fascinating biological implications, the interactions between polymers and surfactants have attracted increasing interest (Faustino, Calado, & Garcia-Rio, 2009; Fumihiko, 1998; Grant, Lee, Liu, & Allen, 2008; Merta, Garamus, Kuklin, Willumeit, & Stenius, 2000; Merta, Torkkeli, Ikonen, Serimaa, & Stenius, 2001; Mészáros, Thompson, Bos, Varga, & Gilányi, 2003; Mészáros, Varga, & Gilányi, 2005; Varga, Mészáros, Makuška, Claesson, & Gilányi, 2009; Vongsetskul et al., 2009; Wang & Tam, 2002; Wang, Li, Li, et al., 2005; Wang, Li, Wang, et al., 2005; Wang, Wang, Wang, & Yan, 2004).

Polyquaternium-10 (PQ-10) is a cationically modified quaternary ammonium derivative of hydroxyethylcellulose (HEC). It is usually formulated together with surfactant in shampoo, cosmetics and abstergents due to its hydrophilicity, biocompatibility and antibacterial characteristics. Up to now, the interactions between PQ-10 and surfactants have been well explored (Lapitsky, Parikh, & Kaler, 2007; Lee & Moroi, 2004; Miyake & Kakizawa, 2002; Winnik, Regismond, & Goddard, 1996; Zhou, Xu, Wang, Golas, & Batteas, 2004), especially the rheological properties (Chronakis & Alexandridis, 2001; Kästner, Hoffmann, Dönges, & Ehrler, 1996; Liu, Yang, Zhang, & Sun, 2010; Patruyo, Müller, & Sáez, 2002; Tsianou & Alexandridis, 1999). Liu et al. (2010) investigated the effect of temperature on the rheological behavior of PQ-10/SDS system and found that the viscosity decreased with increasing temperature. Chronakis and Alexandridis (2001) observed a weaker surfactant concentration dependence of viscosity and a more cross-linked association in the high-MW PQ-10/anionic surfactant systems than in the low-MW ones. Tsianou and Alexandridis (1999) showed that cyclodextrin could disrupt the cross-linked network of PQ-10/SDS system and counteract the viscosity enhancement caused by the surfactant. All these studies revealed that interconnected network structures were formed in the system due to strong interactions between oppositely charged PQ-10 and surfactant. However, the formation of the network has not yet been confirmed by visual measure during the interaction.

The aggregation properties and micropolarity of PQ-10 or hydrophobically modified PQ-10 (LM200)/cationic surfactant systems have been widely studied. Winnik et al. (1996) deduced the presence of low cooperation between LM200 and dodecylammonium bromide (DTAB) from the variation of micropolarity. Burke and Palepu (2001) reported that the aggregation number of alkyltrimethylammonium bromides (C_nTAB, $n = 10$, 12, 14, 16) in LM200 decreased compared with that in pure aqueous solution,

* Corresponding author. Tel.: +86 22 27403475; fax: +86 22 27403475.
E-mail address: ypwei@tju.edu.cn (Y. Wei).

0144-8617/$ – see front matter © 2011 Elsevier Ltd. All rights reserved.
doi:10.1016/j.carbpol.2011.11.081

and the size of the head group had little effect on the aggregation number. Burke, Palepu, Hait, and Moulik (2003) also detected that the aggregation numbers of alkylammonium bromide (C_nAB, n = 10, 12), alkyldimethylammonium bromide (C_nDAB, n = 12) and alkyltrimethylammonium bromides (C_nTAB, n = 10, 12, 14, 16) in PQ-10 medium were similar to that in aqueous solution. However, to our knowledge, only Lee and Moroi (2004) studied the aggregation number of PQ-10/anionic surfactant system. They predicted that the aggregation number for the PQ-10/SDS system increased linearly with SDS concentration and decreased slowly with increasing temperature. In addition, the micropolarity transformation of PQ-10/anionic surfactant systems in the whole phase region (Wang, Kimura, & Dubin, 2000) has also not been examined. In order to gain deeper insights into the cooperative association between PQ-10 and surfactant, much more detailed and systematic investigations on the correlation between the aggregation number and micropolarity will need to be done.

In this paper, the phase behavior of PQ-10/SDBS system was characterized over a large range of mixing ratios by turbidity and visual observation. The critical aggregation concentration (*cac*) and polymer saturation point (*psp*) were estimated by electric conductivity. The micropolarity variation in the whole phase region and the aggregation number were measured by fluorescence. A relation between the aggregation number and micropolarity was also obtained. By combining rheology and TEM, a comprehensive explanation for the viscosity change in this system was provided.

2. Materials and methods

2.1. Materials

PQ-10 (Spec-Chem Industry, China) is cationically modified cellulose ether with an average molecular weight (provided by the manufacture) of 300,000 g/mol and a degree of substitution (from nitrogen content) of 0.37. An aqueous solution of 1% (w/v) PQ-10 bears a charge concentration of 12 mM. Sodium dodecyl benzene sulfonate (SDBS, 95%) was obtained from Aladdin (China). PQ-10 and SDBS were both dried at 60 °C under vacuum before use. Pyrene (98%, Acros Organics) and benzophenone (99%, Alfa Aesar) were used as received. Redistilled water was used in all experiments.

2.2. Methods

2.2.1. Sample preparation

Various PQ-10/SDBS samples were prepared by mixing required amounts of PQ-10 and SDBS aqueous stock solutions together. All the solutions were left to stand for at least 72 h before analysis. The physical appearances of the solutions were examined visually and recorded.

2.2.2. Turbidimetric titration

The turbidity of the PQ-10/SDBS solution, reported as 100-%T, was measured at 420 nm using a UV–vis spectrophotometer in 1-cm-thick quartz sample cells at 25 °C. Turbidimetric titration was carried out by adding equal volumes of 143 mM SDBS and 1% (w/v) PQ-10 into a stirred solution of 0.5% PQ-10 solution to keep the polymer concentration constant. All measured values were corrected by subtracting the turbidity of 0.5% PQ-10 solution. Similar procedures were carried out for 0.2%, 0.1% and 0.05% PQ-10 solutions.

2.2.3. Electric conductivity

The electric conductivity measurements were performed on a DDS-11A conductivity meter equipped with platinized platinum electrodes (cell constant = 1.008 cm^{-1}). It was initially calibrated with KCl standard solution. The PQ-10/SDBS solutions were prepared according to Section 2.2.1, and they were put into a thermostated water bath at 25 °C during measurements.

2.2.4. Steady-state fluorescence measurement

The steady-state fluorescence measurements were carried out using a Cary Eclipse fluorescence spectrophotometer. Pyrene (2.5×10^{-6} M) was used as the probe, benzophenone (1.5×10^{-4} M) was used as the quencher. In this experiment, the concentration of PQ-10 was fixed, but the concentration of SDBS was variable. Samples with precipitates were centrifuged at 12,000 rpm for 20 min to remove the precipitates. Pyrene was excited at 335 nm. The emission spectra were scanned from 350 to 450 nm. The excitation and emission band slits were 5 nm and 2.5 nm, respectively. All the measurements were conducted at 25 °C.

The value of I_1/I_3 in the fluorescence spectrum of pyrene was used to estimate the micropolarity of the solutions. I_1 was also used to determine the aggregation number in quenching experiments. For the PQ-10/SDBS system at the surfactant concentrations (C_s) above the critical aggregation concentration (*cac*), the aggregation number of surfactant per aggregate (N_s) (Panmai, Prud'homme, Peiffer, Jockusch, & Turro, 2002) was calculated from the following equation

$$N_s = \frac{(C_s - cac)\ln(I_0/I)}{[\text{quencher}]}$$

where I_0 and I were the fluorescence intensities without and with quencher, respectively.

2.2.5. Steady shear rheological measurement

The steady shear rheological measurement was performed at 25 °C by using an AR2000 rheometer (TA Instrument, USA) with geometry of flat plate (stainless steel 40 mm radius). AR2000 rheometer was in a mode of stress controlled. The shear rates used here were from 0.001 to 1000 s^{-1}. The apparent viscosity of the PQ-10/SDBS solution was recorded as a function of shear rate.

2.2.6. Transmission electron microscopy

The microstructure of the PQ-10/SDBS system was observed using a FEI Tecnai G2 transmission electron microscope at an acceleration voltage of 200 kV. A small drop of sample solution was placed on the surface of a TEM copper grid and dried at atmospheric pressure. Samples were also prepared by staining with phosphotungstic acid.

3. Results and discussion

3.1. Phase behavior

The phase behavior of PQ-10/SDBS mixtures was studied upon addition of increasing amounts of SDBS while keeping the polymer concentration constant (PQ-10 concentration: 0.05%, 0.1%, 0.2% and 0.5%). The SDBS concentration dependences of turbidity were presented in Fig. 1(A). For PQ-10/SDBS mixtures at 0.05%, 0.1% and 0.2% PQ-10, the turbidity kept nearly constant (<1) until C_0, beyond which the turbidity started to increase slowly. When the SDBS concentration reached C_1, the turbidity increased drastically, and obtained a maximum value at C_2. Then the turbidity decreased, and finally became constant again beyond C_3. For 0.5% PQ-10/SDBS mixture, the turbidity increased from the beginning and the C_0 value was not detected. Values of C_0, C_1, C_2 and C_3 were listed in Table 1.

The C_0 value corresponded to the critical concentration for the onset of complex formation. Below C_0, there were no micelle-like aggregates on the polymer chains (Matsuda & Annaka, 2008; Wang, Li, Li, et al., 2005), and the solutions were still clear. There were slight differences in the C_0 values (0.20 mM, 0.20 mM and 0.29 mM

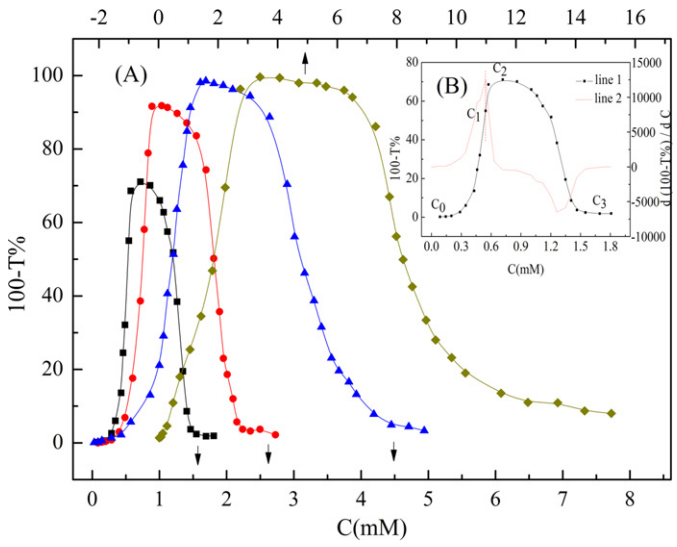

Fig. 1. (A) Turbidity–SDBS concentration dependence for PQ-10/SDBS mixtures at different PQ-10 concentrations (%, w/v): ■, 0.05%; ●, 0.1%; ▲, 0.2%; ♦, 0.5%. (B) The determination of C_0, C_1, C_2, and C_3. Line 2 in (B) is the differentiation of line 1.

for 0.05%, 0.1% and 0.2% PQ-10 solutions, respectively). Increasing the SDBS concentration to C_1, the solutions turned to be quite cloudy, and then showed as two distinct phases, a precipitate and a supernatant. The abrupt increase of turbidity was caused by the formation of precipitation. C_1 was considered as the starting point of precipitation. It could be identified more precisely by differentiating the turbidity curve, as demonstrated in Fig. 1(B). C_1 was determined as the concentration at the maximum of the differential curve. C_1 increased from 0.55 mM to 2.27 mM when the PQ-10 concentration increased from 0.05% to 0.5%. This could be explained that SDBS primarily interacted with PQ-10 by the electrostatic interaction between sulfonic acid groups and quaternary ammonium groups (Abhijit, Soumen, & Satya, 2010), and precipitation

Table 1
Critical concentrations for PQ-10/SDBS mixtures in water.[a]

PQ-10 concentration	C_0	C_1	C_2	C_3
Turbidity				
0.05	0.20	0.55	0.63	1.72
0.1	0.20	0.77	0.92	2.50
0.2	0.29	1.29	1.69	4.71
0.5	–	2.27	3.41	14.35
PQ-10 concentration		*cac*		*psp*
Conductivity				
0.05		0.46		0.72
0.1		0.46		0.86
0.2		0.34		1.09
0.5		0.23		1.52

[a] PQ-10 concentration is given in % (w/v), C_0, C_1, C_2, C_3, *cac* and *psp* are given in mM.

appeared near the charge neutralization point (Miyake & Kakizawa, 2002). Thus, higher concentration PQ-10 required more surfactants to neutralize the cationic charges. After the turbidity reached maximum at C_2, precipitates began to dissolve and the solution was clear again beyond C_3. C_2 increased from 0.63 mM to 3.41 mM and C_3 increased from 1.72 mM to 14.35 mM with increasing PQ-10 concentration from 0.05% to 0.5%. The interval between C_1 and C_3 was the precipitation region (liquid–solid phase separation).

Phase diagrams for the PQ-10/SDBS system were shown in Fig. 2. Each diagram consisted of two single phase domains and two phase separation ones. The first and the second single phase domain corresponded to the surfactant-poor and surfactant-rich mixtures, respectively. The phase separation domains contained a precipitation region where the complex precipitated out and a cloudy region in which insoluble matter dispersed in solutions. The onsets of the precipitation regions determined by observation coincided with the values of C_1 determined by turbidity titration above. And the precipitation domain broadened out significantly for mixtures at higher PQ-10 concentration (0.57–1.72 mM for 0.05% PQ-10, and 2.30–17.22 mM for 0.5% PQ-10). Coacervation (liquid–liquid

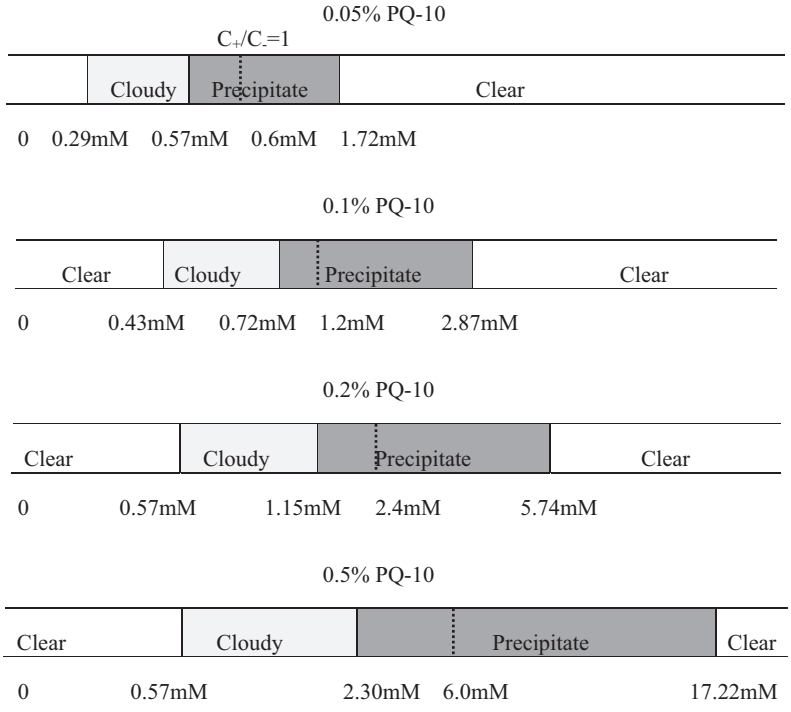

Fig. 2. Phase diagrams for PQ-10/SDBS complexes. The dashed line represented the charge neutrality point.

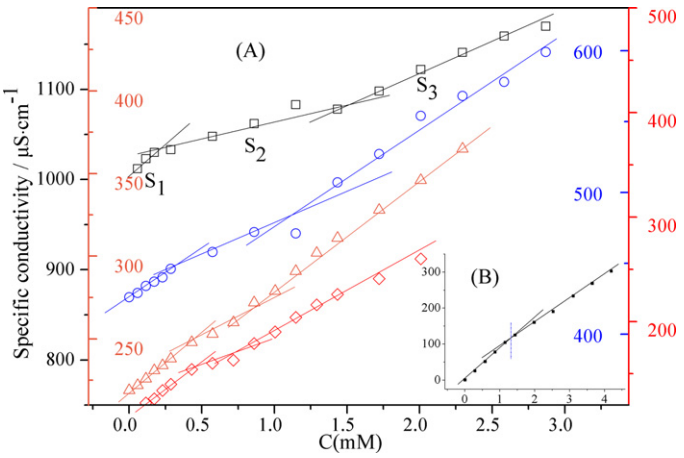

Fig. 3. (A) Specific conductivity–SDBS concentration dependence for PQ-10/SDBS systems at different PQ-10 concentrations (%, w/v): ◊, 0.05%; △, 0.1%; ○, 0.2%; □, 0.5%. (B) Specific conductivity–surfactant concentration dependence for pure SDBS.

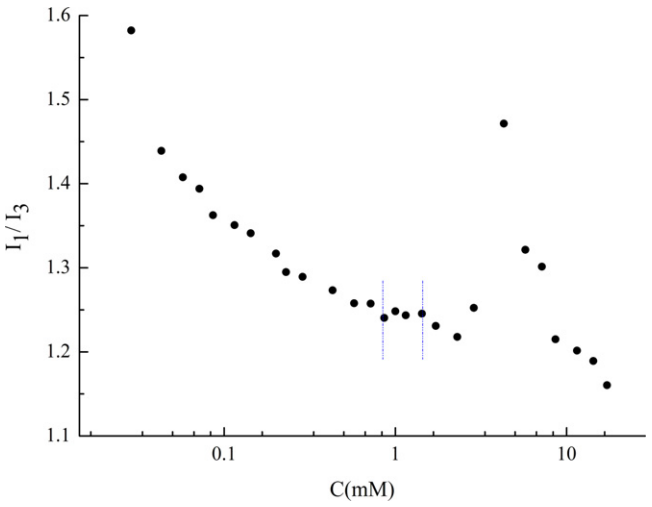

Fig. 4. Dependence of micropolarity on SDBS concentration for 0.5% PQ-10/SDBS solution.

phase separation) was observed in the concentration range of 0.29–0.72 mM for 0.5% PQ-10/SDBS system.

3.2. Electric conductivity

The specific conductivity profiles of SDBS in the presence or absence of PQ-10 were illustrated in Fig. 3(A) and (B), respectively. The *cmc* value of pure SDBS determined at the breaking point was 1.32 mM, which was very close to the reported literature (Greshman, 1957). All the specific conductivity curves for PQ-10/SDBS mixtures in Fig. 3(A) exhibited three linear regions or two breaks, a typical characteristic behavior of polymer/anionic surfactant mixtures (Ali, Suhail, Ghosh, Kamil, & Din, 2009; Faustino et al., 2009; Ghosh, 2005; Ghosh & Banerjee, 2002; Minatti & Zanette, 1996; Ruzza, Froehner, Minatti, Nome, & Zanette, 1994; Witte & Engberts, 1987; Zanette, Ruzza, Froehner, & Minatti, 1996). The first break was called as *cac*, and the second one was denoted as *psp*. The *cac* and *psp* values at different PQ-10 concentrations were listed in Table 1. The *cac* value decreased from 0.46 mM to 0.23 mM while the *psp* value increased from 0.72 mM to 1.52 mM with increasing PQ-10 concentration from 0.05% to 0.5%.

As shown in Fig. 3(A) and (B), the absolute values of the specific conductivity of PQ-10/SDBS systems were higher than that of pure SDBS over the whole range of concentrations. And at the same concentration of SDBS, the specific conductivity increased with the PQ-10 concentration. These results were attributed to that the specific conductivity was related to the dissociated cations and anions of polymer and surfactant. The higher mobility of Na^+ ions of SDBS in PQ-10/SDBS complexes than in SDBS micelles might result in the higher specific conductivity (Khan, Samanta, Ojha, & Mandal, 2008; Winnik, Bystryak, & Chassenieux, 2000). In addition, counterions Cl^- of PQ-10 also contributed to the higher specific conductivity (Pi et al., 2006). Furthermore, it was observed that for PQ-10/SDBS mixtures the slope in the three linear regions was in the order of $S_1 > S_2$ and $S_3 > S_2$, where S_1, S_2 and S_3 were the slope in the first, second and third linear region, respectively. This might result from the highly viscous nature of the solutions as well as the counterion association by the aggregates (Hait, Majhi, Blume, & Moulik, 2003).

3.3. Micropolarity and the aggregation number

The variation of I_1/I_3 with SDBS concentration in 0.5% PQ-10/SDBS solution was depicted in Fig. 4. The I_1/I_3 value of PQ-10 was about 1.7 (similar to the value of pure water), indicating no hydrophobic microdomain formed in the solution. With addition of surfactant, the I_1/I_3 ratio of the mixture began to decrease at the very start. Pure PQ-10 had a relative elongated shape because of the repulsive electrostatic interaction between positive charges along the polyelectrolyte chains (Pi et al., 2006). When surfactant (below *cac*) was added, hydrophobic microdomains started to form in the solution due to the electrostatic attraction between negatively charged surfactant and positively charged polyelectrolyte, and the polymer chains tended to be more curly and compact (Yoshimura, Nagata, & Esumi, 2004). Once the surfactant concentration arrived at *cac*, micelle-like aggregates formed on the polymer chains. Therefore, the I_1/I_3 ratio declined from 1.58 to 1.24 when the concentration increased from 0.03 mM to 0.86 mM. But as the SDBS concentration increased to 0.86 mM, I_1/I_3 stopped declining and remained nearly constant until 1.43 mM. In this flat region, the formation of the micelle-like structures completed (Pi et al., 2006), pyrene was situated in the same microenvironment surrounded by alkyl tails of the micelles. Hence the micropolarity of the solution kept invariant. After the flat region, the value of I_1/I_3 decreased, which implied a more tight arrangement of alkyl tails in the micelles. The I_1/I_3 value began to increase at 2.87 mM and reached a maximum at 4.30 mM. The micropolarity increase derived from the appearance of precipitate. With further addition of surfactant, the precipitate dissolved again and the I_1/I_3 value decreased. Similar phenomenon was observed by Pi et al. (2006).

The aggregation numbers of SDBS (N_s) in 0.5% PQ-10/SDBS mixtures with different SDBS concentrations were summarized in supplementary data. N_s increased from 3 to 13 when the SDBS concentration increased from 0.43 mM to 0.86 mM, suggesting the growth in size of micelle-like aggregates. As a result, the micropolarity decreased in this domain. N_s remained nearly constant (from 13 to 15) in the concentration range of 0.86–1.43 mM, which located in the flat region of the micropolarity curve. The increase of surfactant could only contribute to increasing the number of the aggregate but not its size. With further addition of the surfactant, N_s increased from 15 to 29 and the micelles became more compact. This might be attributed to the less binding sites of the polyelectrolyte, and excessive surfactants entered into the existing micelle to make lager complex but not to induce a new one (Pi et al., 2006). Therefore, the micropolarity of the solution declined again.

3.4. Steady shear rheology and TEM

The shear rate-apparent viscosity curves for 1% PQ-10/SDBS system at various surfactant concentrations were given in Fig. 5.

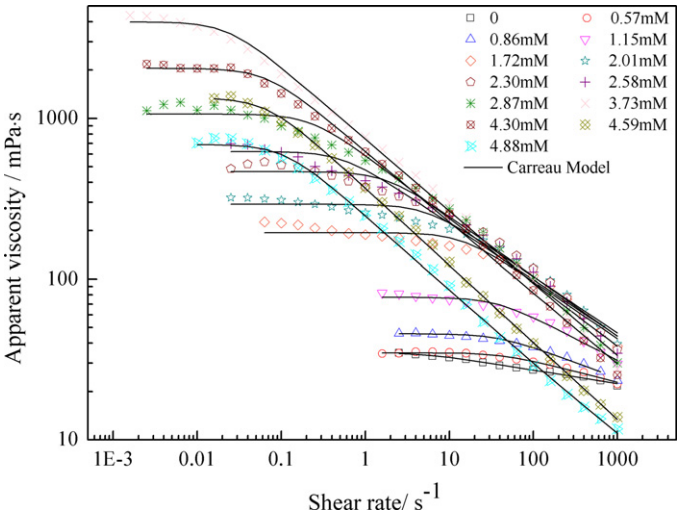

Fig. 5. Shear rate–apparent viscosity curves for 1% PQ-10/SDBS system at various SDBS concentrations.

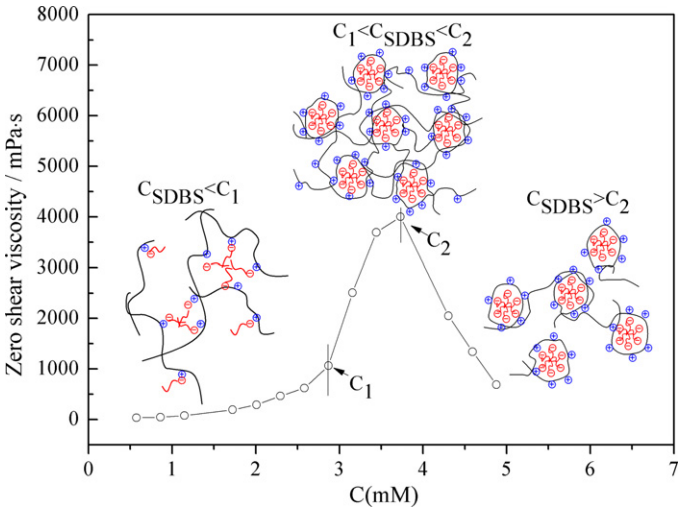

Fig. 6. Dependence of zero shear viscosity on SDBS concentration for 1% PQ-10/SDBS system.

Initially, the apparent viscosity increased with the increase of SDBS concentration as shown in Fig. 5. Simultaneously, the critical shear rate for shear thinning shifted gradually to lower value. After reaching a maximum at 3.73 mM, the apparent viscosity began to decrease. Meanwhile, the critical shear rate shifted to higher value.

The zero shear viscosity (η_0) was plotted against the SDBS concentration in Fig. 6. The TEM images of 1% PQ-10/SDBS mixtures with different SDBS concentrations were presented in Fig. 7. By combining the two figures, the macroscopic rheological properties and microscopic cooperative binding could be correlated. As shown in Fig. 7(a), the polymer exhibited fibril-like morphology in the absence of SDBS, and the corresponding η_0 value was ~34 mPa s. When SDBS was added (the concentration of SDBS was lower than 2.87 mM), η_0 increased slowly, and branched wormlike structures appeared as revealed by Fig. 7(b) and (c). Firstly, SDBS molecules bound to quaternary ammonium sites on the polymer chains by strong electrostatic force. Then, with increasing of SDBS concentration, the micellization of electrostatic-bound surfactant monomers occurred. In the meantime, more polymer chains were associated together by hydrophobic associate of dodecylbenzene chains of SDBS. When the concentration of SDBS increased to 2.87 mM (denoted by C_1 in Fig. 6), η_0 increased sharply, and reached maximum (~4000 mPa s) at 3.73 mM (designated as C_2 in Fig. 6). Network structures were observed in this domain ($C_1 < C_{SDBS} < C_2$) and the density increased with increasing SDBS concentration as found in Fig. 7(d) and (e). It was indicated that the onset of formation of the network structures coincided with the origin of the sharp increase of η_0. Moreover, the maximum value of η_0 corresponded to the highest density of the network. These results suggested that the abrupt viscosity increase mainly arose from the formation of interconnected networks. In addition, the critical shear rate for shear thinning decreased with increasing density of the network. More compact network required more time to regain equilibrium when subjected to certain shear stress, thus shear thinning would occur earlier

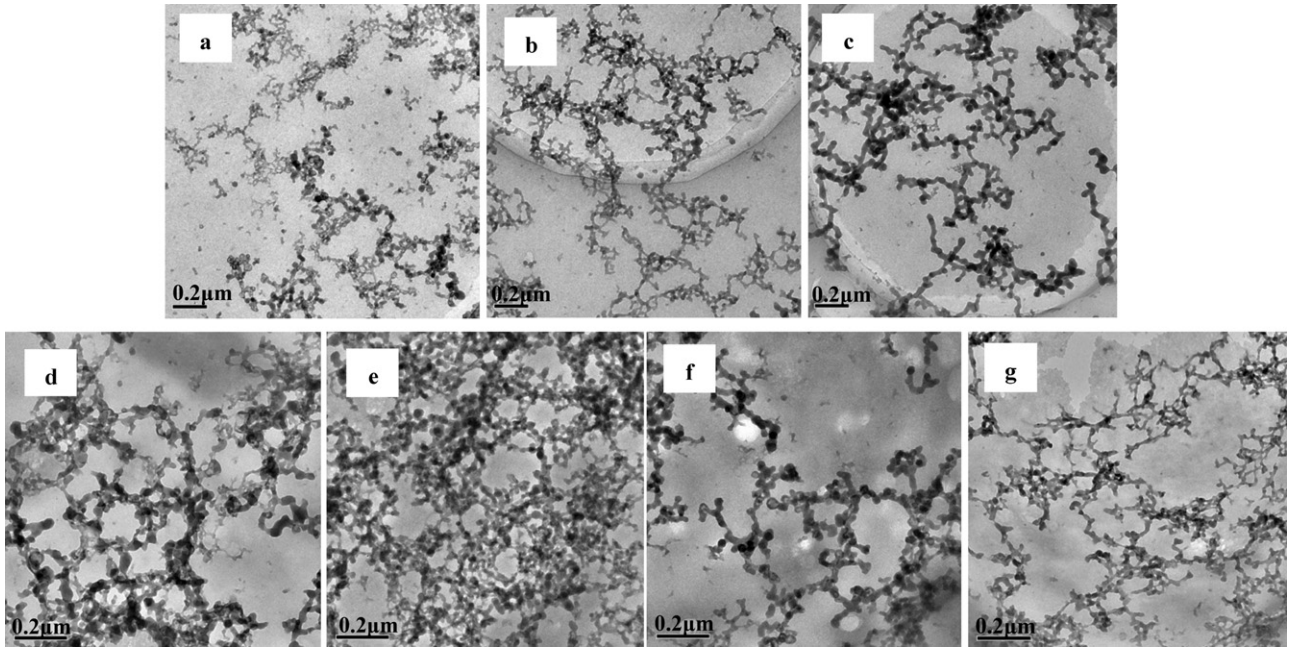

Fig. 7. TEM images for 1% PQ-10/SDBS complexes at various surfactant concentrations: (a) 0, (b) 0.06 mM, (c) 1.72 mM, (d) 2.87 mM, (e) 3.73 mM, (f) 4.02 mM, and (g) 4.59 mM.

(Sharma, Shrestha, Varade, & Aramaki, 2007). As the SDBS concentration was beyond C_2, η_0 decreased drastically. The density of the network became lower and the cross-linked network gradually broke down as seen in Fig. 7(f) and (g). Further addition of surfactant increased the charge density of surfactant micelles along the polymer chains, and eventually produced strong intermicellar and intercomplex electrostatic repulsion (Wang, Kimura, Huang, & Dubin, 1999), which made the network collapse and PQ-10/SDBS complexes disintegrate into small complexes. Therefore, the viscosity decreased.

4. Conclusion

The phase behavior, solution properties and microstructure of oppositely charged polymer surfactant system composed of cationic cellulose (PQ-10) and anionic surfactant (SDBS) were examined. A correlation between the micropolarity and the aggregation number of PQ-10/SDBS mixtures was established by fluorescence. The aggregation number maintained growth as the micropolarity decreased and kept constant when the micropolarity remained invariant. Rheological research indicated that the viscosity of the mixtures increased firstly and then decreased rapidly with increasing surfactant concentration. TEM showed the formation and collapse of network structures in the mixtures, which corresponded to the viscosity increase and decease, respectively.

Appendix A. Supplementary data

Supplementary data associated with this article can be found, in the online version, at doi:10.1016/j.carbpol.2011.11.081.

References

Abhijit, D., Soumen, G., & Satya, P. M. (2010). Interaction of cationic hydroxyethylcellulose (JR400) and cationic hydrophobically modified hydroxyethylcellulose (LM200) with the amino-acid based anionic amphiphile sodium n-dodecanoyl sarcosinate (SDDS) in aqueous medium. *Carbohydrate Polymers*, *80*, 44–52.

Ali, M. S., Suhail, M., Ghosh, G., Kamil, M., & Din, K. U. (2009). Interactions between cationic gemini/conventional surfactants with polyvinylpyrrolidone: Specific electric conductivity and dynamic light scattering studies. *Colloids and Surfaces A: Physicochemical and Engineering Aspects*, *350*, 51–56.

Burke, S. E., & Palepu, R. (2001). Interactions of a hydrophobically modified cationic cellulose ether derivative with amphiphiles of like charge in an aqueous environment. *Carbohydrate Polymers*, *45*, 233–244.

Burke, S. E., Palepu, R. M., Hait, S. K., & Moulik, S. P. (2003). Physicochemical investigations on the interaction of cationic cellulose ether derivatives with cationic amphiphiles in an aqueous environment. *Progress in Colloid and Polymer Science*, *122*, 47–55.

Chavanpatil, M. D., Khdair, A., Patil, Y., Handa, H., Mao, G., & Panyam, J. (2007). Polymer–surfactant nanoparticles for sustained release of water-soluble drugs. *Journal of Pharmaceutical Sciences*, *96*, 3379–3389.

Chronakis, I. S., & Alexandridis, P. (2001). Rheological properties of oppositely charged polyelectrolyte–surfactant mixtures: Effect of polymer molecular weight and surfactant architecture. *Macromolecules*, *34*, 5005–5018.

Faustino, C. M. C., Calado, A. R. T., & Garcia-Rio, L. (2009). Gemini surfactant–protein interactions: Effect of pH, temperature, and surfactant stereochemistry. *Biomacromolecules*, *10*, 2508–2514.

Fumihiko, T. (1998). Polymer–surfactant interaction in thermoreversible gels. *Macromolecules*, *31*, 384–393.

Ghosh, S. (2005). Physicochemical and conformational studies of papain/sodium dodecyl sulfate system in aqueous medium. *Colloids and Surfaces A: Physicochemical and Engineering Aspects*, *264*, 6–16.

Ghosh, S., & Banerjee, A. (2002). A multitechnique approach in protein/surfactant interaction study: Physicochemical aspects of sodium dodecyl sulfate in the presence of trypsin in aqueous medium. *Biomacromolecules*, *3*, 9–16.

Grant, J., Lee, H., Liu, R. C. W., & Allen, C. (2008). Intermolecular interactions and morphology of aqueous polymer/surfactant mixtures containing cationic chitosan and nonionic sorbitan esters. *Biomacromolecules*, *9*, 2146–2152.

Greshman, J. W. (1957). Physico-chemical properties of solutions of para long chain alkylbenzenesulfonates. *The Journal of Physical Chemistry*, *61*, 581–584.

Hait, S. K., Majhi, P. R., Blume, A., & Moulik, S. P. (2003). A critical assessment of micellization of sodium dodecyl benzene sulfonate (SDBS) and its interaction with poly(vinyl pyrrolidone) and hydrophobically modified polymers, JR400 and LM 200. *The Journal of Physical Chemistry B*, *107*, 3650–3658.

Kästner, U., Hoffmann, H., Dönges, R., & Ehrler, R. (1996). Interactions between modified hydroxyethyl cellulose (HEC) and surfactants. *Colloids and Surfaces A: Physicochemical and Engineering Aspects, 1996*, *112*, 209–225.

Khan, M. Y., Samanta, A., Ojha, K., & Mandal, A. (2008). Interaction between aqueous solutions of polymer and surfactant and its effect on physicochemical properties. *Asia-Pacific Journal of Chemical Engineering*, *3*, 579–585.

Lapitsky, Y., Parikh, M., & Kaler, E. W. (2007). Calorimetric determination of surfactant/polyelectrolyte binding isotherms. *The Journal of Physical Chemistry B*, *111*, 8379–8387.

Lee, J., & Moroi, Y. (2004). Investigation of the interaction between sodium dodecyl sulfate and cationic polymers. *Langmuir*, *20*, 4376–4379.

Liu, Y. H., Yang, R. M., Zhang, J. X., & Sun, J. H. (2010). Rheological and self-assembly behavior of cationized hydroxycellulose with ionic surfactants. *Fibers and Polymers*, *11*, 744–748.

Matsuda, T., & Annaka, M. (2008). Salt effect on complex formation of neutral/polyelectrolyte block copolymers and oppositely charged surfactants. *Langmuir*, *24*, 5707–5713.

Mel'nikov, S. M, Sergeyev, V. G., & Yoshikawa, K. (1995). Transition of double-stranded DNA chains between random coil and compact globule states induced by cooperative binding of cationic surfactant. *Journal of the American Chemical Society*, *117*, 9951–9956.

Merta, J., Garamus, V. M., Kuklin, A. I., Willumeit, R., & Stenius, P. (2000). Determination of the structure of complexes formed by a cationic polymer and mixed anionic surfactants by small-angle neutron scattering. *Langmuir*, *16*, 10061–10068.

Merta, J., Torkkeli, M., Ikonen, T., Serimaa, R., & Stenius, P. (2001). Structure of cationic starch (CS)/anionic surfactant complexes studied by small-angle X-ray scattering (SAXS). *Macromolecules*, *34*, 2937–2946.

Mészáros, R., Thompson, L., Bos, M., Varga, I., & Gilányi, T. (2003). Interaction of sodium dodecyl sulfate with polyethyleneimine: Surfactant-induced polymer solution colloid dispersion transition. *Langmuir*, *19*, 609–615.

Mészáros, R., Varga, I., & Gilányi, T. (2005). Effect of polymer molecular weight on the polymer/surfactant interaction. *The Journal of Physical Chemistry B*, *109*, 13538–13544.

Minatti, E., & Zanette, D. (1996). Salt effects on the interaction of poly(ethylene oxide) and sodium dodecyl sulfate measured by conductivity. *Colloids and Surfaces A: Physicochemical and Engineering Aspects*, *113*, 237–246.

Miyake, M., & Kakizawa, Y. (2002). Study on the interaction between polyelectrolytes and oppositely charged ionic surfactants: Solubilized state of the complexes in the postprecipitation region. *Colloid and Polymer Science*, *280*, 18–23.

Nilsson, S., Goldraich, M., Lindman, B., & Talmon, Y. (2000). Novel organized structures in mixtures of a hydrophobically modified polymer and two oppositely charged surfactants. *Langmuir*, *16*, 6825–6832.

Panmai, S., Prud'homme, R. K., Peiffer, D. G., Jockusch, S., & Turro, N. J. (2002). Interactions between hydrophobically modified polymers and surfactants: A fluorescence study. *Langmuir*, *18*, 3860–3864.

Patruyo, L. G., Müller, A. J., & Sáez, A. E. (2002). Shear and extensional rheology of solutions of modified hydroxyethyl celluloses and sodium dodecyl sulfate. *Polymer*, *43*, 6481–6493.

Pi, Y. Y., Shang, Y. Z., Peng, C. J., Liu, H. L., Hu, Y., & Jiang, J. W. (2006). Interactions between gemini surfactant alkanediyl-α,ω-bis(dodecyldimethylammonium bromide) and polyelectrolyte NaPAA. *Journal of Colloid and Interface Science*, *301*, 631–636.

Ruzza, Â. A., Froehner, S. J., Minatti, E., Nome, F., & Zanette, D. (1994). Quantitative treatment of ketal hydrolysis in aqueous solutions containing polymer–surfactant complexes using a pseudophase kinetic model. *The Journal of Physical Chemistry*, *98*, 12361–12366.

Scherlund, M., Brodin, A., & Malmsten, M. (2000). Nonionic cellulose ethers as potential drug delivery systems for periodontal anesthesia. *Journal of Colloid and Interface Science*, *229*, 365–374.

Sharma, S. C., Shrestha, R. G., Varade, D., & Aramaki, K. (2007). Rheological behavior of gemini-type surfactant/alkanolamide/water systems. *Colloids and Surfaces A: Physicochemical and Engineering Aspects*, *305*, 83–88.

Tsianou, M., & Alexandridis, P. (1999). Control of the rheological properties in solutions of a polyelectrolyte and an oppositely charged surfactant by the addition of cyclodextrins. *Langmuir*, *15*, 8105–8112.

Varga, I., Mészáros, R., Makuška, R., Claesson, P. M., & Gilányi, T. (2009). Effect of graft density on the nonionic bottle brush polymer/surfactant interaction. *Langmuir*, *25*, 11383–11389.

Vongsetskul, T., Taylor, D. J. F., Zhang, J., Li, P. X., Thomas, R. K., & Penfold, J. (2009). Interaction of a cationic gemini surfactant with DNA and with sodium poly(styrene sulphonate) at the air/water interface: A neutron reflectometry study. *Langmuir*, *25*, 4027–4035.

Wang, C., & Tam, K. C. (2002). New insights on the interaction mechanism within oppositely charged polymer/surfactant systems. *Langmuir*, *18*, 6484–6490.

Wang, X. Y., Li, Y. J., Li, J. X., Wang, J. B., Wang, Y. L., Guo, Z. X., et al. (2005). Salt effect on the complex formation between polyelectrolyte and oppositely charged surfactant in aqueous solution. *The Journal of Physical Chemistry B*, *109*, 10807–10812.

Wang, X. Y., Li, Y. J., Wang, J. B., Wang, Y. L., Ye, J. P., & Yan, H. K. (2005). Interactions of cationic gemini surfactants with hydrophobically modified poly(acrylamides) studied by fluorescence and microcalorimetry. *The Journal of Physical Chemistry B*, *109*, 12850–12855.

Wang, X. Y., Wang, J. B., Wang, Y. L., & Yan, H. Y. (2004). Salt effect on the complex formation between cationic gemini surfactant and anionic polyelectrolyte in aqueous solution. *Langmuir*, *20*, 9014–9018.

Wang, Y. L., Kimura, K., & Dubin, P. L. (2000). Polyelectrolyte-micelle coacervation: Effects of micelle surface charge density, polymer molecular weight, and polymer/surfactant ratio. *Macromolecules*, *33*, 3324–3331.

Wang, Y. L, Kimura, K., Huang, Q. R., & Dubin, P. L. (1999). Effects of salt on polyelectrolyte-micelle coacervation. *Macromolecules*, *32*, 7128–7134.

Winnik, F. M., Regismond, S. T. A., & Goddard, E. D. (1996). Interactions of cationic surfactants with a hydrophobically modified cationic cellulose polymer: A study by fluorescence spectroscopy. *Colloids and Surfaces A: Physicochemical and Engineering Aspects*, *106*, 243–247.

Winnik, M. A., Bystryak, S. M., & Chassenieux, C. (2000). Study of interaction of poly(ethylene imine) with sodium dodecyl sulfate in aqueous solution by light scattering, conductometry, NMR, and microcalorimetry. *Langmuir*, *16*, 4495–4510.

Witte, F. M., & Engberts, J. B. F. N. (1987). Perturbation of SDS and CTAB micelles by complexation with poly(ethy1ene oxide) and poly(propy1ene oxide). *The Journal of Organic Chemistry*, *52*, 4767–4772.

Yoshimura, T., Nagata, Y., & Esumi, K. (2004). Interactions of quaternary ammonium salt-type gemini surfactants with sodium poly(styrene sulfonate). *Journal of Colloid and Interface Science*, *275*, 618–622.

Zanette, D., Ruzza, Â. A., Froehner, S. J., & Minatti, E. (1996). Polymer–surfactant interactions demonstrated by a kinetic probe: Degree of ionization. *Colloids and Surfaces A: Physicochemical and Engineering Aspects*, *108*, 91–100.

Zhou, S. Q., Xu, C., Wang, J., Golas, P., & Batteas, J. (2004). Phase behavior of cationic hydroxyethyl cellulose–sodium sodecyl sulfate mixtures: Effects of molecular weight and ethylene oxide side chain length of polymers. *Langmuir*, *20*, 8482–8489.